C.P. No. 430
(20,306)
A.R.C. Technical Report

C.P. No. 430
(20,306)
A.R.C. Technical Report

MINISTRY OF SUPPLY

AERONAUTICAL RESEARCH COUNCIL

CURRENT PAPERS

Some Experiments with Static Tubes at Transonic Speeds in a Slotted-Wall Wind Tunnel

by

E.W.E. Rogers, M.Sc., and I.M. Hall, Ph.D.,
of the Aerodynamics Division, N.P.L.

LONDON: HER MAJESTY'S STATIONERY OFFICE

1959

Price 3s. 6d. net

C.P. No. 430

Some Experiments with Static Tubes at Transonic Speeds in a Slotted-Wall Wind Tunnel

- By -
E. W. E. Rogers, M.Sc.
and I. M. Hall, Ph.D.
of the Aerodynamics Division, N.P.L.

August, 1958

E R R A T A

Text

p.3, penultimate para., "$\neq$" should read "$\pm$"

p.4, §.4, *l*.4, insert hyphen in "over-expansion"

" §.5, *l*.5, move comma to end of brackets

Figures

Fig. 2 Labels should read (a) $M_o = 0.801$ (b) $M_o = 0.903$

Fig.4(b) should read (increased sensitivity and horizontal cut-off)

Fig.5 (i) It has not been possible to put in all the points in the region $0.95 < M_o < 0.975$ due to the fact that many points are superimposed on those already marked.

(ii) L.H. Label - line omitted.

(iii) Legend - blockage of A is 0.204%, B 0.0086% and C 0.0048%

Fig.6 " " " "

Fig.9 Bottom right-hand corner - should be "tests^3"

Fig.11 Arrow for bow-wave instability should point downwards into trough.

CF

C.P. No. 430

Some Experiments with Static Tubes at Transonic Speeds in a Slotted-Wall Wind Tunnel

- By -
E. W. E. Rogers, M.Sc.
and I. M. Hall, Ph.D.
of the Aerodynamics Division, N.P.L.

14th July, 1958

SUMMARY

Some results obtained with five static tubes at transonic speeds in an N.P.L. slotted wall tunnel (17" x 14" working section) are discussed. The effect of model size is considered, and a comparison made with free-flight tests, for tubes having a hemi-spherical nose.

A brief analysis is made of the flow development with stream Mach number, and of the problems associated with shock-wave reflection.

1. Introduction

In recent years there have been several investigations of the characteristics of static tubes at subsonic and supersonic speeds, and the effects of changes in stream Mach number and incidence have been studied in wind-tunnel tests and free-flight experiments.

At transonic speeds less information is available, one reason for this being the presence of tunnel interference effects at stream Mach numbers near unity, which distort the flow field around the model. The nature of the interference depends on the type of transonic working section and also the size of the model relative to that of the working section. Thus by testing similar models of different size in the same working section, some assessment can be made of the way the interference effects become important.

The present note is concerned with results obtained from four nearly-similar models of the Mark IXA pitot-static head (using only the static orifices) which has a hemispherical nose, and also from another small static tube having an ogival nose. It thus supplements the earlier work reported by Roe in Ref.1.

The tests were carried out at intervals between 1956 and 1958.

2. Experimental Details

2.1 Static tubes

Four models, of different sizes, representing the Mark IXA pitot-static head were tested and the relevant dimensions are given in Fig.1.

The/

The largest model (A) was in fact a full-scale head, with pitot opening and two banks of static slots situated at 8.0 and 8.7 tube diameters from the nose. No pitot measurements were made during the present tests. The tapered portion of the tube[4] differed from that used with full-scale flight instruments, though the degree of taper was the same.

In the three smaller models of this type (B, C and D), there was no pitot opening and the six circumferential static slots were replaced by four equally-spaced circular holes, at about 8.6 tube diameters from the nose. The three models were not exactly similar however, as can be seen from the dimensions given in Fig.1. Downstream of the static holes, each tube was parallel for about 12 diameters, and then tapered slowly to represent approximately the boom attachment of the flight instrument. Some 50 diameters from the nose was a circular collar, originally intended to simulate the effect of the wing leading edge or fuselage nose. All three models were considerably smaller than model A, as is shown in Table 1.

To obtain some information on the effects of changing the nose shape, tests were also made with a standard tunnel static tube (similar to that used for tunnel calibration, flow exploration, etc). This tube (E) was about the same size as D and had four static holes placed 22 diameters behind the pointed ogival nose.

The relative sizes of these five models is set out in Table 1, which also gives the blockage of each model. This is defined as the ratio of the tube cross-sectional area at the static openings to the cross-sectional area of the transonic working section (17" high, 14" wide).

Table 1

Model Type	Mark IXA-type Models				Tunnel Static Tube
Designation	A	B	C	D	E
Tube diameter / Full-scale tube diameter	1.0	0.215	0.160	0.103	-
% blockage	0.204	0.0086	0.0048	0.0021	0.0021
Reynolds number at $M_o = 1$, based on tube diameter ($\times 10^{-5}$)	2.97	0.64	0.48	0.31	0.31

2.2 The tunnel working section

The transonic working section of the 18" x 14" tunnel is described in detail in Ref.2. The 14" wide walls have longitudinal slots, one-eleventh of the width being open to the plenum chamber. The sidewalls are formed by interchangeable panels (glass in steel frames).

2.3 Experimental method

Each model was mounted on the tunnel traverse gear, which was itself supported by a bar extending from the sidewall downstream from the end of the slotted working section. In this way the support bar interfered as little as possible with the flow in the working section.

The/

The models were aligned along the tunnel axis, care being taken to ensure that the static holes or slots were at precisely the same position in the tunnel for all models.

The static pressure measured by the model was read on a water manometer against the pressure from a reference hole on the tunnel wall some distance upstream from the model position. This wall reference hole was later calibrated (in the absence of the model) against another wall hole on a slat immediately above the position normally occupied by the model static holes. Finally the tunnel static tube was used to measure the pressure variation across the tunnel between the model position and the second wall hole; this was small, but not negligible, and enabled a more accurate assessment to be made of the 'true' static pressure in the empty tunnel at the model position.

The experimental values of static pressure were reduced to coefficient form in the following manner:-

$$C_p = \frac{p_{\text{measured by tube}} - p_{\text{'true' static}}}{(\frac{1}{2}\rho U^2)_{\text{appropriate to 'true' static}}} .$$

Appropriate corrections were also applied to the nominal stream Mach number.

The static pressure measurements were supplemented by an extensive set of schlieren flow photographs, and in the case of tube A, by some surface oil-flow patterns. The Mach number range covered was from 0.6 to 1.2.

3. Results

3.1 Presentation of results

At moderate subsonic speeds, where blockage effects are small, all five tubes might be expected to have the same value of C_p. This was not so (Table 2).

Table 2

Tube	A	B	C	D	E
C_p at $M_o = 0.801 (C_{p_o})$	+0.0129	+0.0123	+0.0264	+0.0055	-0.0055

The experimental error is estimated to be about ± 0.001 in C_p at $M_o = 1$.

The comparatively large value of C_{p_o} obtained with the full-size tube (A) is similar to that reported by Mabey[3] from R.A.E. tests on another full-size instrument. The variation in the results obtained with tubes B, C and D is more likely to be associated with small imperfections in the models* rather than with Reynolds number changes. The difference in C_{p_o} between tubes D and E is probably due to the more rearward position of the static hole position on the latter model (see Fig.1). A second tunnel static tube, similar in shape to tube E, but having static holes at 33 diameters from the nose gave a value of C_{p_o} of -0.0067.

The/

---

*Refs. 4 and 5 suggest that the actual shape of the static orifice may be important in determining the value of the pressure reading.

The present tests, however, were less concerned with the absolute calibration of the models than with the static pressure variation with Mach number, and thus it was decided to work in terms of the static pressure increment ΔC_p, where at any stream Mach number

$$\Delta C_p = C_p - C_{p_o}.$$

3.2 Results from tube A

In order to assist in the understanding of the way in which the transonic flow is modified by model scale, it is necessary to consider in some detail the development of the flow pattern with Mach number about tube A.

Shock waves were first detected (using a sensitive schlieren system) close to the shoulder of the model at a stream Mach number of 0.70, and this value is in good agreement with the critical Mach number (0.69) obtained by Cole[7] from pressure-plotting tests on a hemi-spherically-nosed body. A well defined shock pattern is not established until nearly $M_o = 0.9$. Below this Mach number numerous small shocks occur just downstream from the shoulder (Fig.2(a)), a region where the corresponding oil-flow pattern suggests a band of locally separated flow. This reattaches as a relatively thick turbulent boundary layer.

Similar schlieren and oil patterns for $M = 0.903$ are shown in Fig.2(b). The flow pattern contains three main shock waves, as sketched in Fig.3. The front inclined shock is associated with the over expansion of the surface flow around the nose and is a marked feature of transonic and supersonic flow over blunt bodies of revolution. The second inclined shock system may originate from the transition to turbulent flow within the separated flow region, close to reattachment. At high subsonic speeds, this shock (or series of shocks) may alternatively be the result of reflections from the model surface of incoming compressions, which themselves originated from expansion waves from the nose reflecting from the sonic boundary. The third shock is nearly normal to the stream and terminates the local supersonic region.

With further increase in stream Mach number, the terminal shock moves rearward and becomes dish-shaped, becoming normal to the stream close to and far from the model surface. Due to the axi-symmetrical nature of the flow, the outer normal region appears on schlieren photographs as a straight line, (behind the true terminal shock) and superficially resembles yet another shock extending to the model surface (see Fig.4(b) for example).

The outer part of the terminal shock reaches both the glass sidewalls and the slotted walls of the tunnel at a stream Mach number of approximately 0.96 (see Fig.4(c)).

The proximity of the supersonic flow to the wall is likely to distort the flow field around the model, and in particular the position of the sonic line. Hence the strength of the reflected compressions reaching the model will be altered, thus affecting the shock strength, and rate of movement.

The effect must be present both before and after the terminal shock reaches the tunnel walls, but seems to be most serious in the latter condition. As will be shown in §3.3.1 (and Fig.5), the effect of increasing blockage is to slow down the rate at which the terminal shock moves rearward. The exact reasons for this are not clear at present, and in addition to the modification of shock strength mentioned above, it is probable that the downstream pressure behind terminal shock is affected by model size through the agency of the plenum chamber. Further information on this point is being sought.

With/

Near M_o = 0.994 (Fig.4(c)), the terminal shock is inclined when it strikes the slotted and glass walls. The intersection trace on the latter is therefore slightly curved. The flow behind this shock is still, of course, subsonic and no reflection of the terminal wave occurs.

By M_o = 1.02, the inclined shock wave resulting from the combining of several weaker inclined waves has reached and is reflected from, both sets of walls. These reflections (compressions) interact with the terminal shock; because the tunnel is rectangular (and not square) the intersections from the two pairs of walls take place at slightly different positions on the tube. The terminal shock is again dished, this time with the concave side towards the oncoming stream; its significance in relation to the interference-free flow about the model is debatable, but its movement can be regarded as a measure of interference effects. The double image of the hyperbola-like intersection of the front-inclined shock with the sidewalls in Fig.4(g) and elsewhere is due to the model being slightly off centre between the glass walls.

With further increase in stream Mach number the degenerate terminal shock continues to move rearward, but with decreasing strength. At M_o = 1.049 (Fig.4(g)) the shock is about to pass over the foremost row of static slots. The bow wave is now visible. Near M_o = 1.07, the reflection of the front-inclined shock intersects the model surface just ahead of the terminal shock (but behind the static slots), which has now become a series of weak near-normal shocks associated principally with a further reflection of the front-inclined shock. By M_o = 1.08, the terminal shock has disappeared from view and can be regarded merely as the breakdown shock for the combined model-tunnel system.

At slightly supersonic speeds the sonic line is curved towards the oncoming flow. If the subsonic region ahead of the model extends to the tunnel walls the bow shock will not, of course, reflect. Regular, or initially Mach-type, reflection occurs as the subsonic region contracts with increase in stream Mach number, an inclined reflection first becoming visible at about M_o = 1.08. Reflection of the bow-wave as a weak normal shock may occur just before this condition. The reflected bow wave, weak at first, traverses the length of the model as the stream Mach number is increased, and passes over the static slots at about 1.15*. Once this condition has been achieved, the model, regarded as a static tube, can be considered as interference free.

Briefly, then, the three main interference effects observed with tube A are:-

1. Extension of terminal shock to wall and distortion of flow field. This leads to a slowing down of the rearward movement of the terminal shock with increasing stream Mach number.

2. Reflection of the front-inclined shock to intersect with and modify the terminal shock (possibly further affecting its rearward movement), and subsequently to intersect the model.

3. Modification of subsonic flow field between model and bow wave, possibly altering the stand-off distance at low supersonic Mach numbers. Regular reflection becomes possible just after the supersonic flow extends to the wall behind the bow wave. The model can then be subject to the reflections of the bow wave, which increases rapidly in strength as the stream Mach number is raised.

These/

---

*The reflected bow wave from the slotted walls is the second of the two inclined reflected waves in Fig.4(h); the first originates from junctions on the slotted wall liners. The curved trace immediately behind the bow wave is the intersection of this in the glass sidewalls.

These effects will be present in some degree whatever the size of the model. With a very small model, however, the Mach number range over which interference occurs will be very small; the results from the smaller models will now be considered.

3.3 Effect of model size (tubes A to D)

3.3.1 Movement of the terminal shock

Estimated values of the onset of interference effects due to the terminal shock reaching the wall are:-

Tube	A	B	C	D
Stream Mach numbers for onset of interference (M_c)	0.96	0.98	0.99	0.99

Greater accuracy than this is not possible.

Below these Mach numbers, the rearward movement of the terminal shock should be independent of model size; this is reasonably confirmed in Fig.5. The retardation of the rearward movement is further illustrated by the points obtained from the schlieren photographs of tube D, in which this model was offset from the tunnel centreline towards one slotted wall.

Similar results have been obtained before. Fig.5 includes two curves due to Roe[1], for bluff-nosed bodies, of almost identical blockages to the present models A and D. The variation in shock position for a given stream Mach number is much greater in this case.

3.3.2 Interference from the forward inclined shock

Because of the small sizes of models B, C and D, the reflection of the forward inclined shock does not intersect the model until well behind the static holes. This intersection takes place at a stream Mach number of about 1.03 for tubes B and C, and at about 30 and 53 diameters downstream from the nose respectively. The corresponding stream Mach number for tube A is 1.02, only slightly lower. With tube D, the reflected waves never intersect the model surface directly; they interact initially with the bow wave from the boss, which itself forms a rearward limit to the movement of the terminal shock.

Measurements made from the flow photographs suggest that the shape of the forward inclined shock and its reflection are almost independent of model size for models B, C and D, and hence that the position at which the reflection would intersect the model is approximately a constant distance from the nose.

3.3.3 The bow wave

Measurements of the bow wave position from the shoulder of each model is shown in Fig.6. The accuracy of measurement is not very high with the smallest models (C and D), but the results do suggest a slight effect of model size on bow-wave position for stream Mach numbers less than about 1.08. This trend (the bow wave closer to the nose for the smaller blockages) is, however, the opposite to that observed by Roe[1] for bluff-nosed bodies.

The agreement with Moeckel's simple geometric theory[6] is similar to that obtained in Ref.1 and elsewhere.

Instability of the bow-wave position was observed for a very limited range of Mach number (near 1.025) for all four models, and was most pronounced for the two smallest models. This phenomena is thought

to/

to be due to an interaction between the weak bow wave and a stray shock wave originating from one of the tunnel-wall junctions. The bow-wave position at this Mach number is very sensitive to changes in the pressure field, which must be greatly distorted by the extraneous wave.

Typical schlieren photographs near this instability region are shown in Fig.7. At the lower Mach number (1.028) the bow wave appears blurred despite the microsecond exposure. Even when the bow-wave position has become stable, the shape of the wave is still distorted (Fig.7(b)). This distortion lessens as the stream Mach number is further increased.

This effect would be relatively unimportant, except for the fact that the static-pressure readings are affected by the instability (see below).

When the local subsonic region ahead of the model, and behind the bow wave, contracts sufficiently, reflection of the bow wave from the walls can occur. Reflections from the slotted walls were first detected in the schlieren photographs at stream Mach numbers of 1.08 (A), 1.038 (B and C) and 1.015 (D). In these cases it is estimated that the reflected bow wave would intersect the model at 2.2, 18, 37, and 30 diameters from the nose respectively. With static holes near 8.6 diameters, only the readings from model A should be subject to direct interference from the reflected bow wave.

3.3.4 Effect of model size on static pressure observations

The static-pressure change with Mach number for each of the four Mark IXA type tubes is shown in Fig.8.

As the terminal shock approaches the static openings, the static-pressure reading increases due to the reduced velocity behind the shock. The passage of the shock over the openings causes the pressure to fall rapidly; the Mach number at which this occurs is in good agreement with the value deduced from the schlieren photographs (see Fig.5) and thus confirms the dish-like structure of the terminal shock.

The slowing down of the rearward movement of the terminal shock with increasing blockage is clearly shown.

The front-inclined shock and the bow wave, when reflected from the tunnel walls, do not intersect the model ahead of, or at, the static openings, except for tube A, where the bow-wave reflection passes over the static slots near $M_o = 1.15$. Because of the lack of data in this region for this model, the passage of the reflected shock cannot be detected with any certainty.

The bow wave instability region results in a marked rise in the pressure measured by tubes C and D; pressure changes were also observed with tube B, but could not be read with any accuracy. With the largest model, this region occurs before the terminal shock reaches the static slots and no effect on the static reading was noticed.

The other variations in static pressure shown in Fig.8 are probably associated with stray shocks in the working section of the tunnel. Apart from the junction shock mentioned earlier, it is known[2] that some of the sidewall junctions give rise to weak shocks. These cannot be detected easily from the schlieren photographs, particularly at the higher stream Mach numbers when multiple reflections occur.

Ref.3 contains similar curves of static-pressure variation with Mach number for a standard Mark IXA instrument in free-flight, and also for a modified tube with the pitot entry blocked one inch from the nose. These results are shown in Fig.9, together with the corresponding

curve/

curve for model D of the present tests. Agreement between the tunnel and flight tests for the Mach number at which the terminal shock crosses the static holes must be considered as satisfactory, in view of the nature of the comparison.

The magnitude of the observed static-pressure rise (δC_p) due to the shock is greater in the tunnel tests at N.P.L. and R.A.E. than in the flight tests and this pressure rise is plotted in Fig.10 against the blockage. Some additional points due to Roe[1] are included. The points available seem to lie on a single curve, which approaches the free-flight (or zero blockage) results very steeply. The magnitude of δC_p is, of course, mainly a measure of the local Mach number over the forward part of the body and hence indirectly depends on the stream Mach number at which the terminal shock crosses the static openings, which in turn depends on the blockage.

The value of δC_p compared with flight results may however give some indication of the magnitude of the blockage effects, and Fig.10 serves to illustrate how rapidly these become serious.

3.4 Effect of nose shape at constant blockage (tubes D and E)

A comparison of the readings obtained from the two small tubes (D and E) is shown in Fig.11. The static-pressure error for the tube with an ogival nose is small partly because of the smaller disturbance due to this type of nose, and partly because of the more rearward position of the static holes. The terminal shock was first observed on tube E at about $M_o = 0.990$. The front-inclined shock systems are much less marked, and appear to be of little significance.

Bow-wave instability was once again observed and had an appreciable effect on the tube reading. Bow-wave reflection from the slotted walls could be seen at about $M_o = 1.03$, the reflection intersecting the model some 40 diameters from the nose.

4. Concluding Remarks

The simple tests described in this note have enabled some assessment to be made of the effect of model size on the flow field in a transonic tunnel with slotted walls. Even with comparatively small blockages (of the order of 0.01%) some interference effects are large enough to be serious, if extreme precision is required. The most noticeable effect is the delay in the rearward movement of the terminal shock, with a corresponding increase in the pressure rise measured when that shock crosses the static holes. Because of this delay, the large blockage models measure the static pressure correctly (or nearly so) up to a higher stream Mach number (see Fig.8). There appeared to be a slight blockage effect on bow-wave position.

The reflection from the walls of the front inclined shock and the bow wave were found to be serious only for the largest model in the present tests. Because of the small size of models B to E, the reflections tended to intersect the model well downstream from the measuring station. A full investigation of the shock reflection problems associated with the bow wave (particularly at very low supersonic Mach numbers) was precluded by the disturbing influence of stray shocks originating from the tunnel walls. In a limited Mach number range, these were thought to cause an instability in the position of the bow-wave position. By affecting the flow field around the model, this instability caused a rapid alteration of the measured pressure.

The smallest model tested suffered from tunnel interference in a comparatively limited range of Mach number between about $M_o = 0.99$ and 1.015, if the bow-wave instability region is neglected. By comparison, the full-size tube (A) was subject to interference effects in the Mach number range between 0.96 and 1.15.

A/

A more pointed nose was found to delay appreciably the effects due to the movement of the terminal shock, and also to reduce the strength of the front-inclined shock. The more rearward static-hole position was also beneficial, and in the case of tube E, was not sufficiently far downstream to be influenced by the bow-wave reflection when this occurred.

The present results are of course subject to Reynolds number effects, and Ref.3 suggests that these can affect the static pressure rise due to the terminal shock. On the other hand, the results from the smallest models seem consistent with flight data. The position and origin of the front-inclined shock, which might be expected to be influenced by model size changes, is in fact very nearly independent of model size.

5. Acknowledgement

The experimental observations discussed in this note were obtained by Mr. C. J. Berry and Mr. J. Townsend.

References

No.	Author(s)	Title, etc.
1	F. E. Roe	Some aspects of transonic tunnel operation in industry. J.R.Ae.Soc. Vol.62, p.16 January, 1958.
2	I. M. Hall	The operation of the N.P.L. 18 in. × 14 in. wind tunnel in the transonic speed range. C.P. No. 338. January, 1957.
3	D. G. Mabey	The calibration at transonic speeds of a Mark 9A pitot static head with and without flow through the static slots. R.A.E. Technical Note Aero.2500. C.P. No. 384. March, 1957.
4	E. W. E. Rogers	The effects of incidence on two Mark 9A Pitot-static heads at subsonic speeds. A.R.C.18,489. 11th June, 1956.
5	K. Merriam and E. R. Spaulding	Comparative tests of pitot-static tubes. N.A.C.A. TN 546. November, 1935.
6	W. E. Moeckel	Approximate method of predicting the form and location of detached shock waves ahead of plane or axially-symmetric bodies. N.A.C.A. TN 1921. July, 1949.
7	R. I. Cole	Pressure distributions on bodies of revolution at subsonic and transonic speeds. N.A.C.A. RM L52D30 (TIL/3261) July, 1952.

HBF

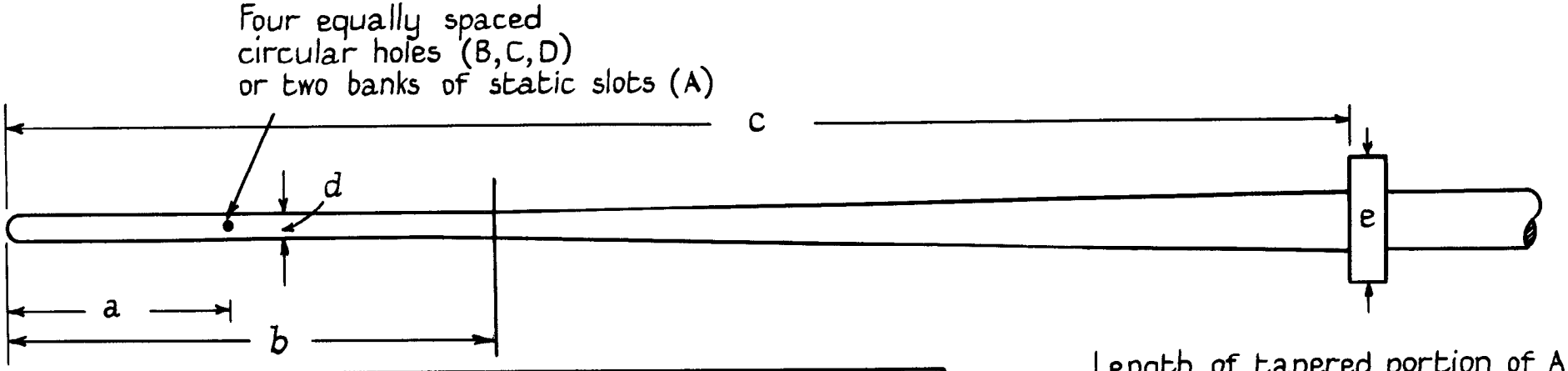

Length of tapered portion of A is 6"

	A	B	C	D
Distance from nose to static holes (a)	6·0 (8·0 d) 6·5 (8·7 d)	1·38 (8·6 d)	1·03 (8·6d)	0·68 (8·8d)
Distance from nose to beginning of taper (b)	14·0 (18·7d)	3·0 (18·6d)	2·5 (20·8d)	1·5 (19·5d)
Distance from nose to collar (c)	No collar	8·38 (52·1d)	6·31 (52·6d)	4·12 (53·5d)
Tube diameter in parallel section (d)	0·75	0·161	0·120	0·077
Collar diameter (e)	No collar	0·768	0·577	0·405

All dimensions in inches.

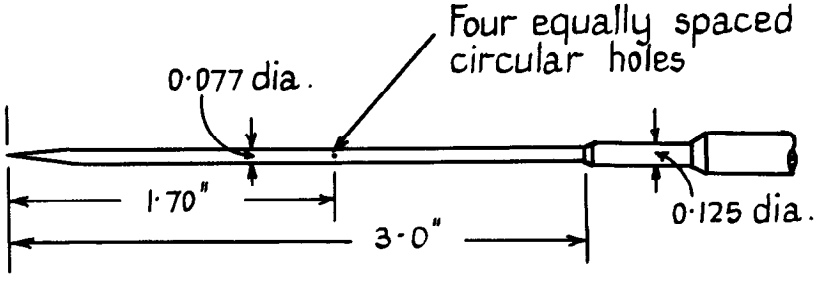

Static holes are placed at 22d from nose.

20,306
Fig. 1.

Details of Mark IX-type and tunnel static tubes.

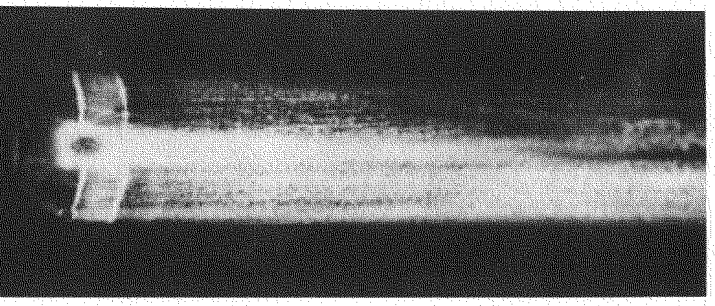

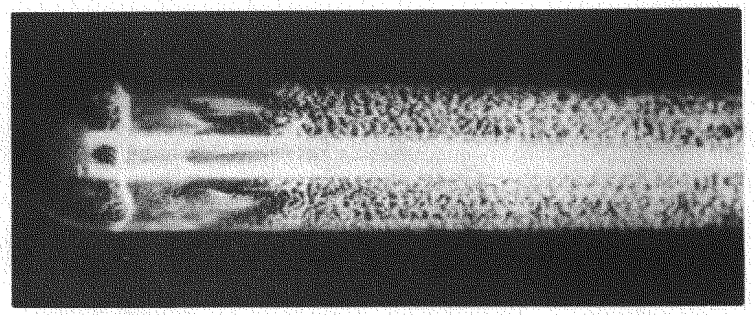

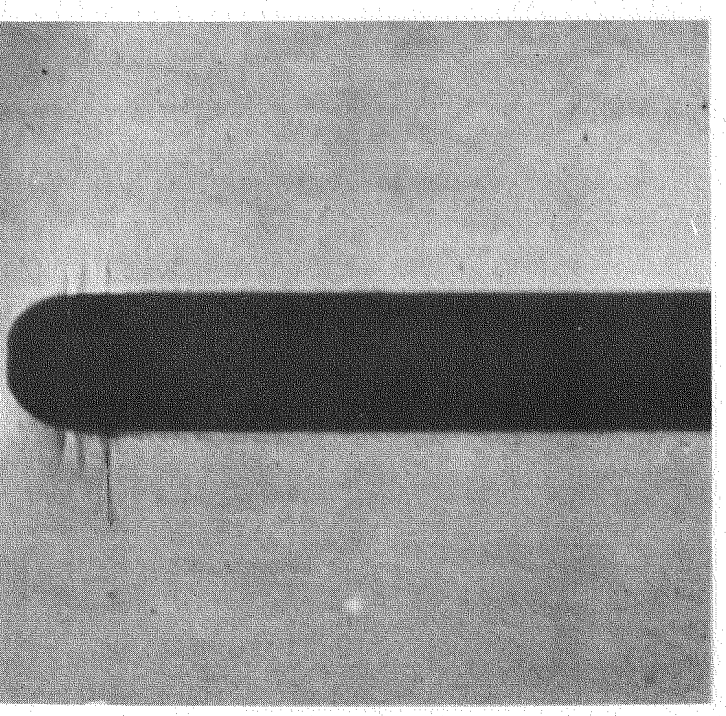

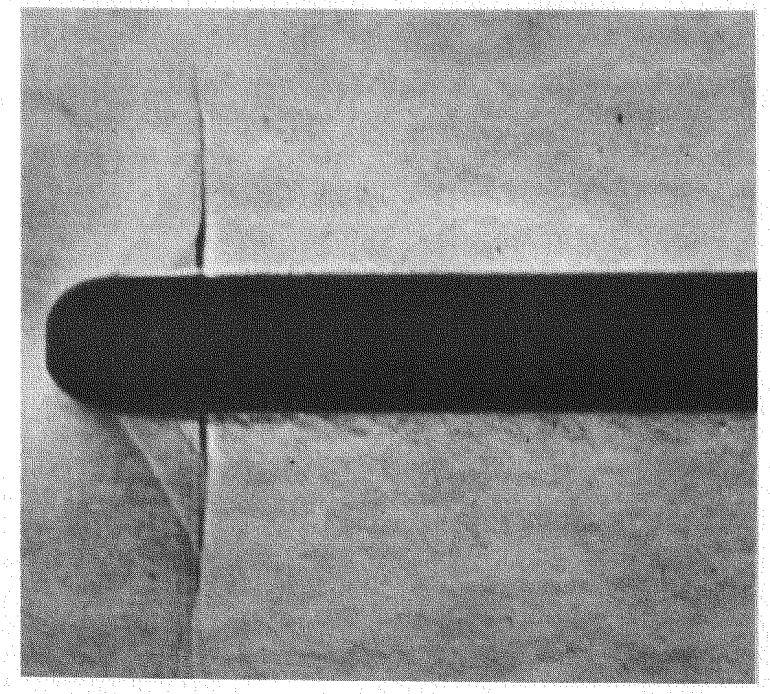

$M_o = 0.801$

$M_o = 0.903$

FIG. 2. Comparison of schlieren and oil flow photographs at subsonic stream speeds (Tube A)

20,306
FIG. 3.

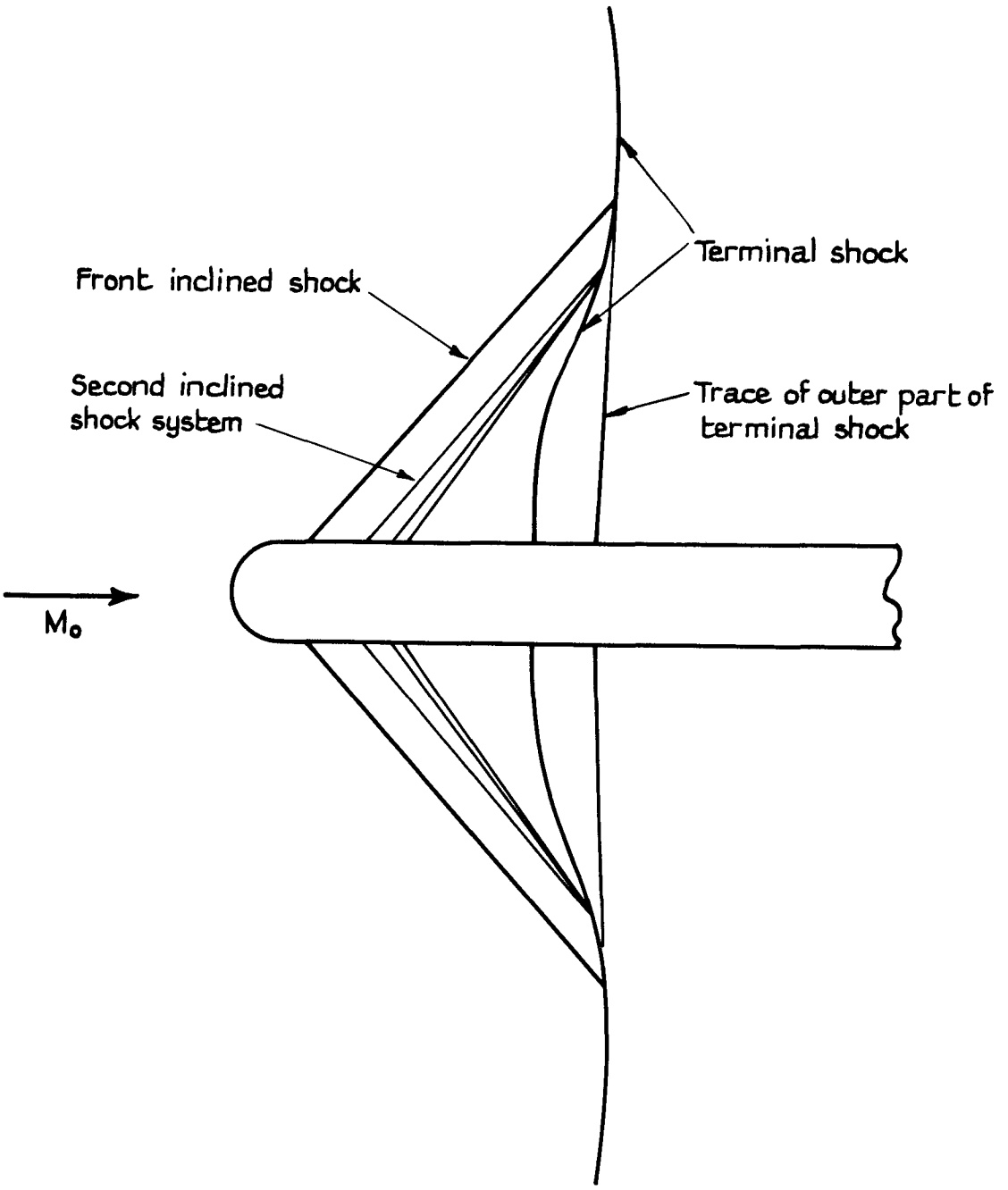

Shockwave pattern of high subsonic speeds

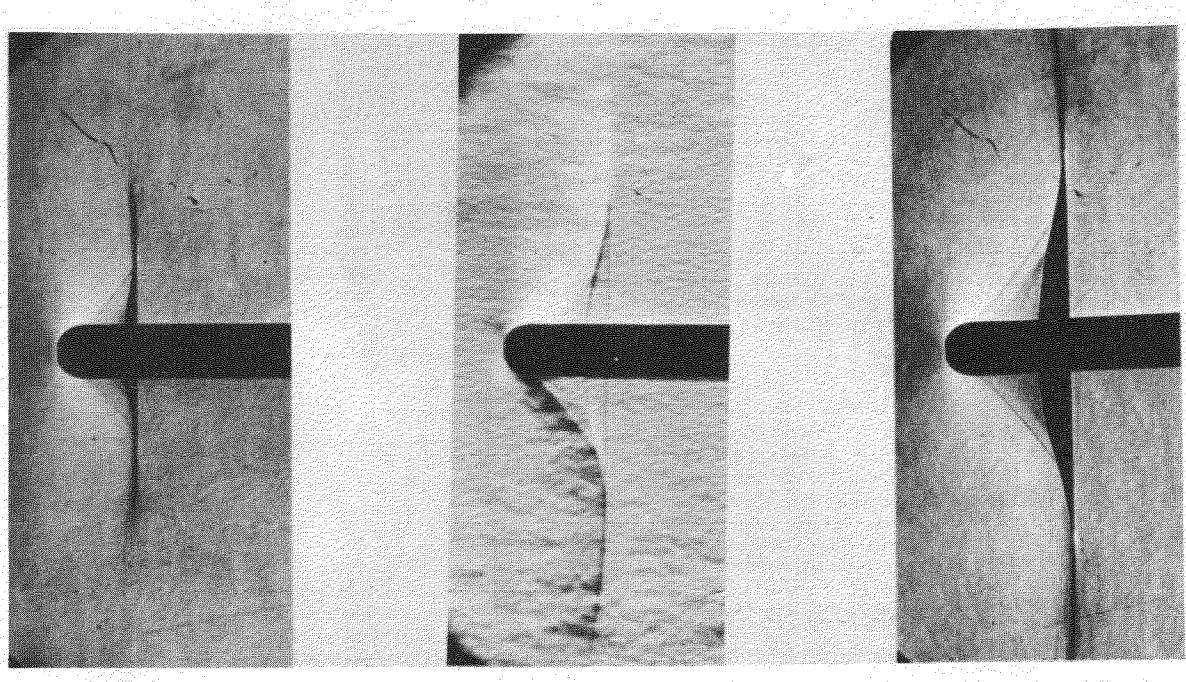

(a) $M_o = 0.934$ (b) $M_o = 0.954$ (increased sensitivity) (c) $M_o = 0.964$

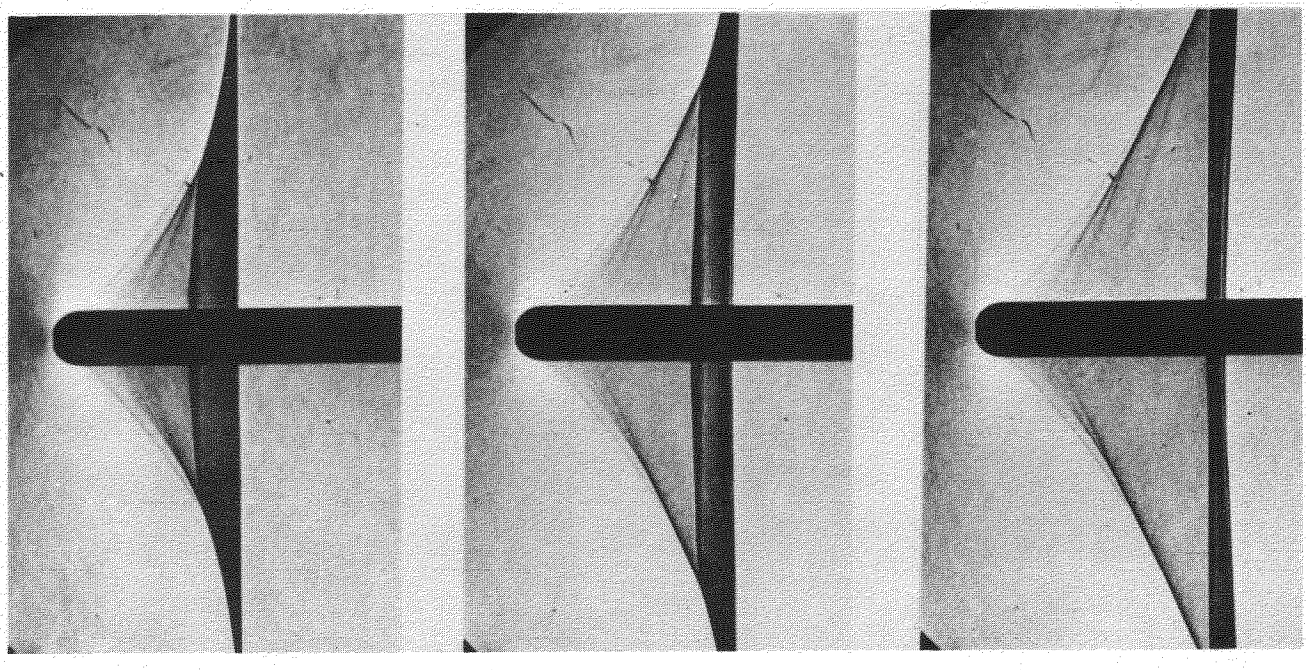

(d) $M_o = 0.984$ (e) $M_o = 0.994$ (f) $M_o = 1.005$

FIG. 4. Development of flow pattern with stream Mach number for Tube A.

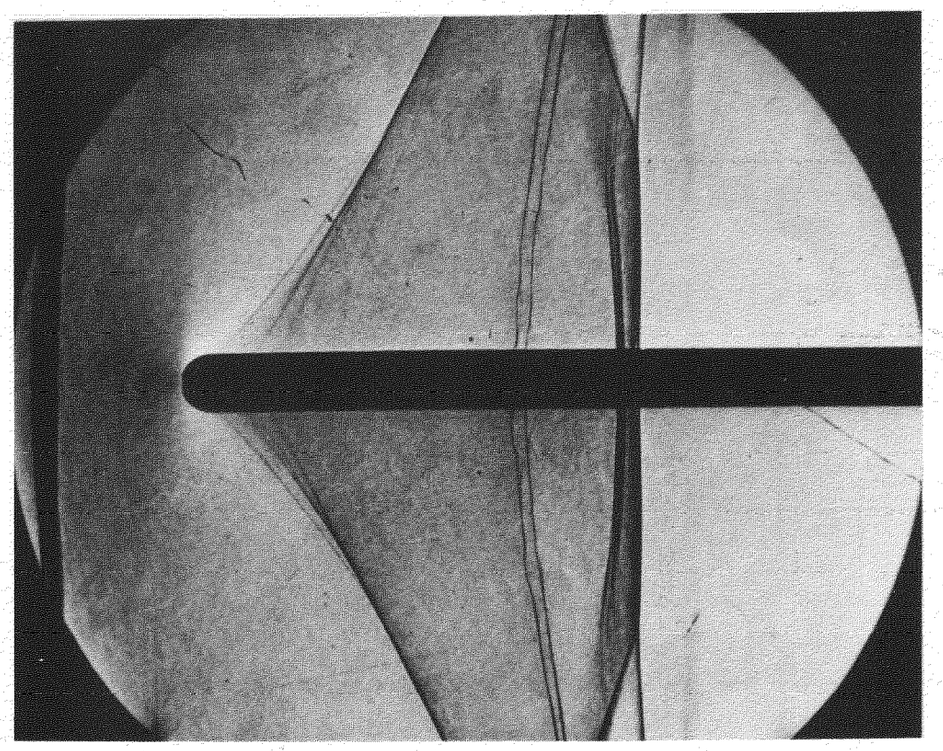

(g) $M_o = 1 \cdot 049$

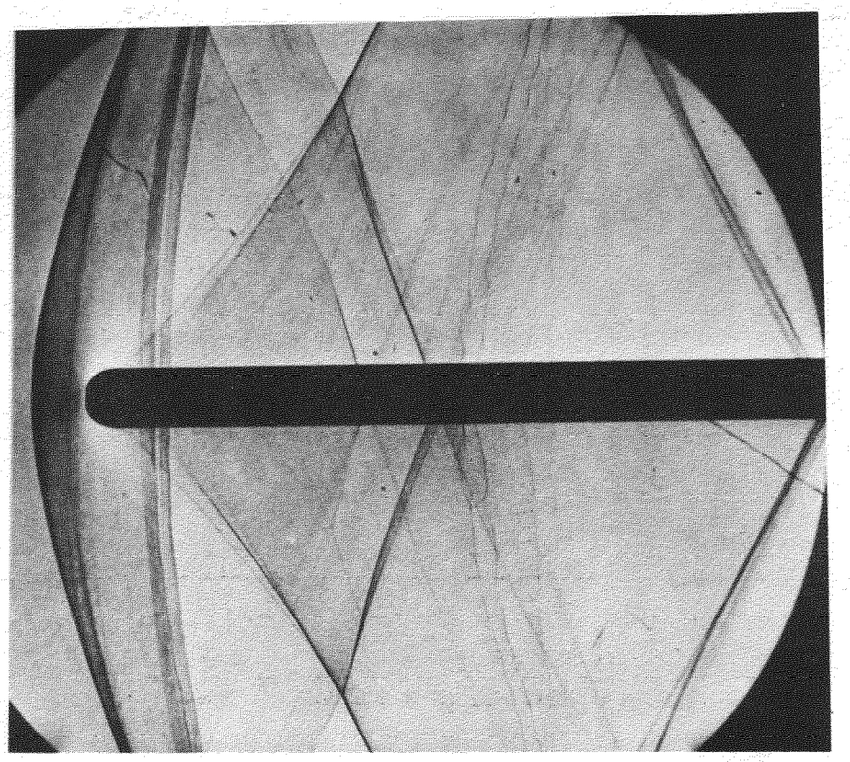

(h) $M_o = 1 \cdot 132$

FIG. 4 (cont)

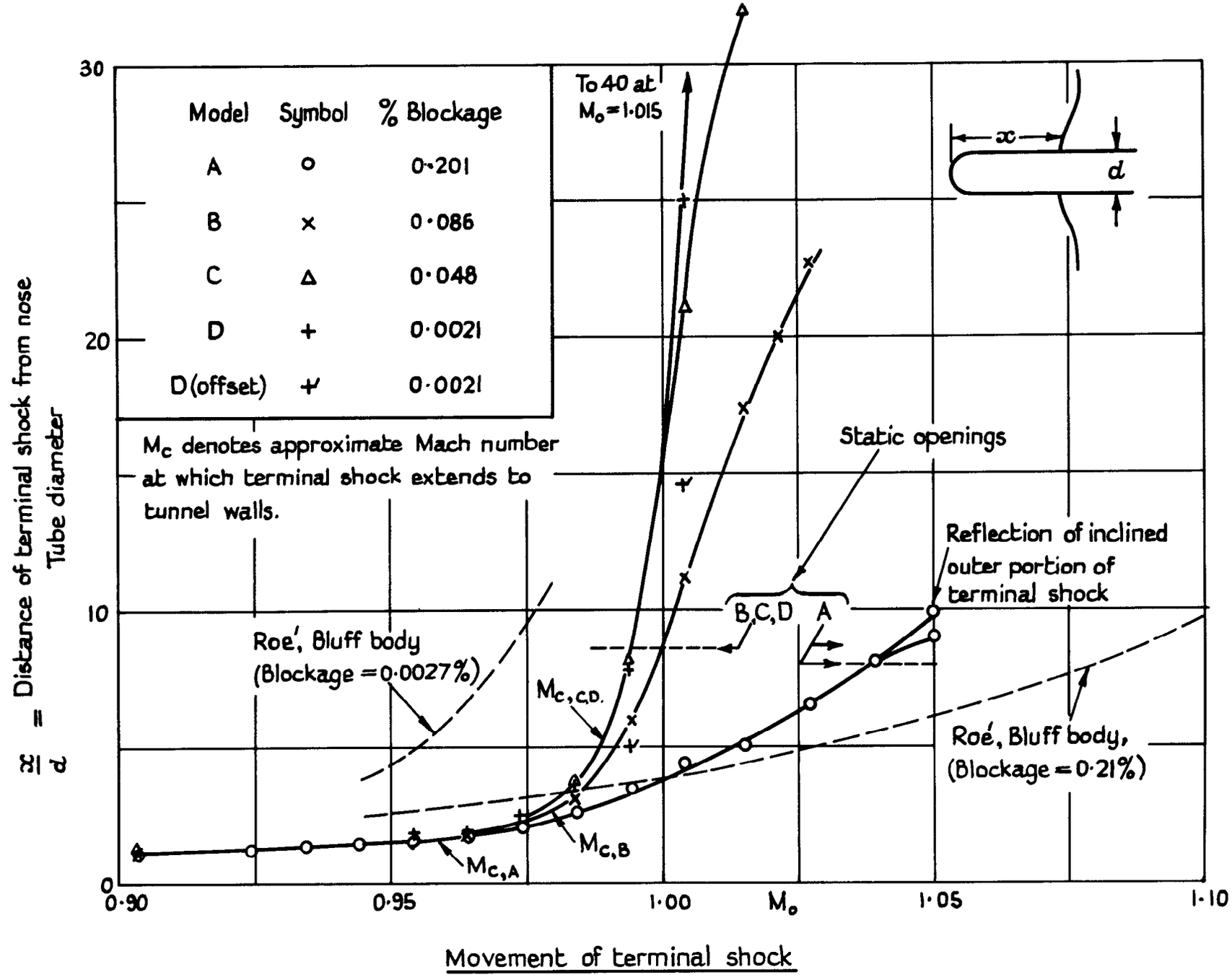
Model Symbol % Blockage
A o 0·201
B × 0·086
C Δ 0·048
D + 0·0021
D(offset) + 0·0021
To 40 at M₀ = 1·015
x
d
Mc denotes approximate Mach number at which terminal shock extends to tunnel walls.
Static openings
Reflection of inclined outer portion of terminal shock
B,C,D
A
Roe', Bluff body (Blockage = 0·0027%)
Mc,C,D.
Roé, Bluff body, (Blockage = 0·21%)
Mc,A
Mc,B
x/d = Distance of terminal shock from nose / Tube diameter
30
20
10
0
0·90
0·95
1·00
M₀
1·05
1·10
Movement of terminal shock

20,306
Fig. 5.

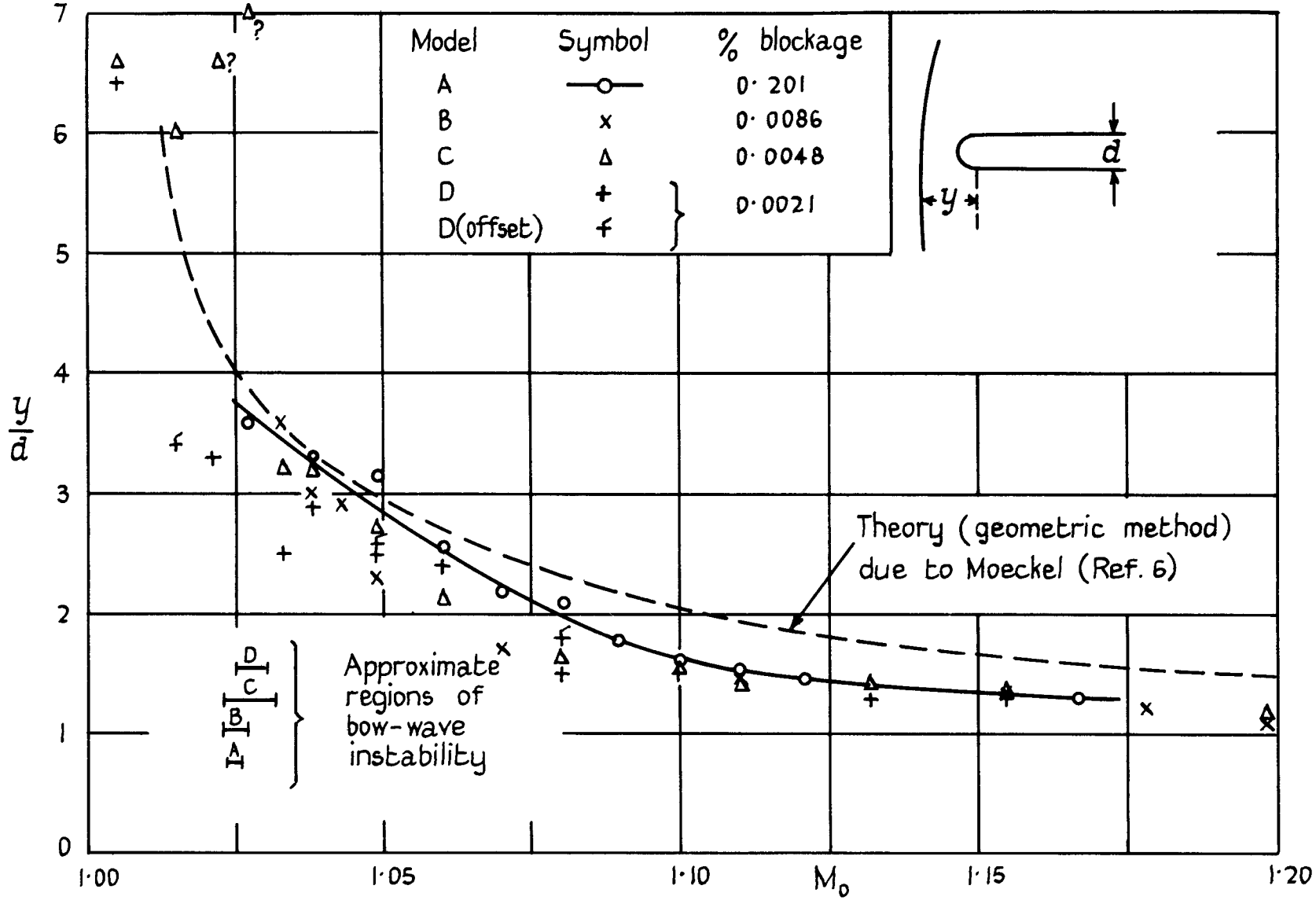

Bow wave position.

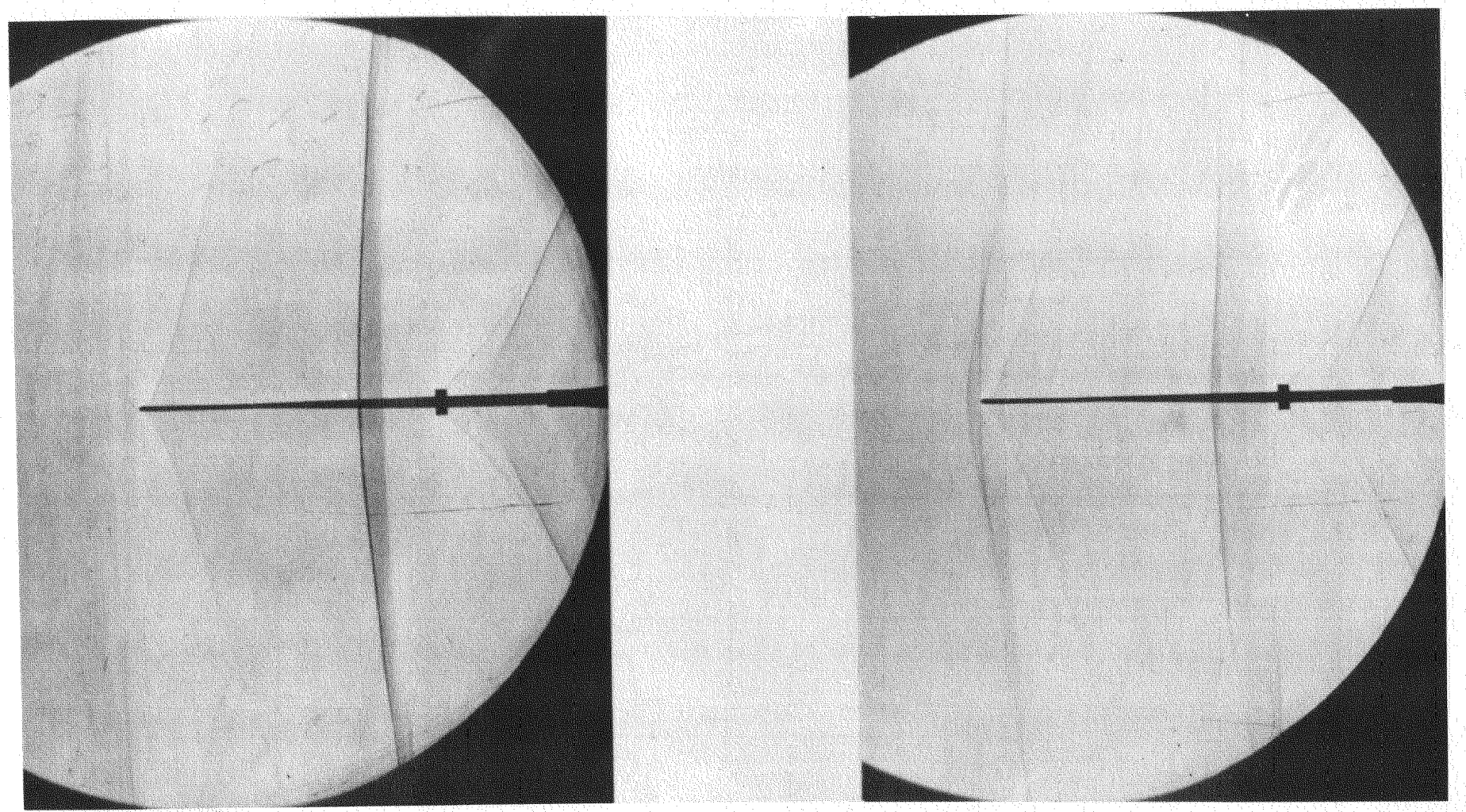

(a) $M_o = 1 \cdot 028$ (b) $M_o = 1 \cdot 033$

FIG. 7. Bow-wave instability and distortion (Tube D)

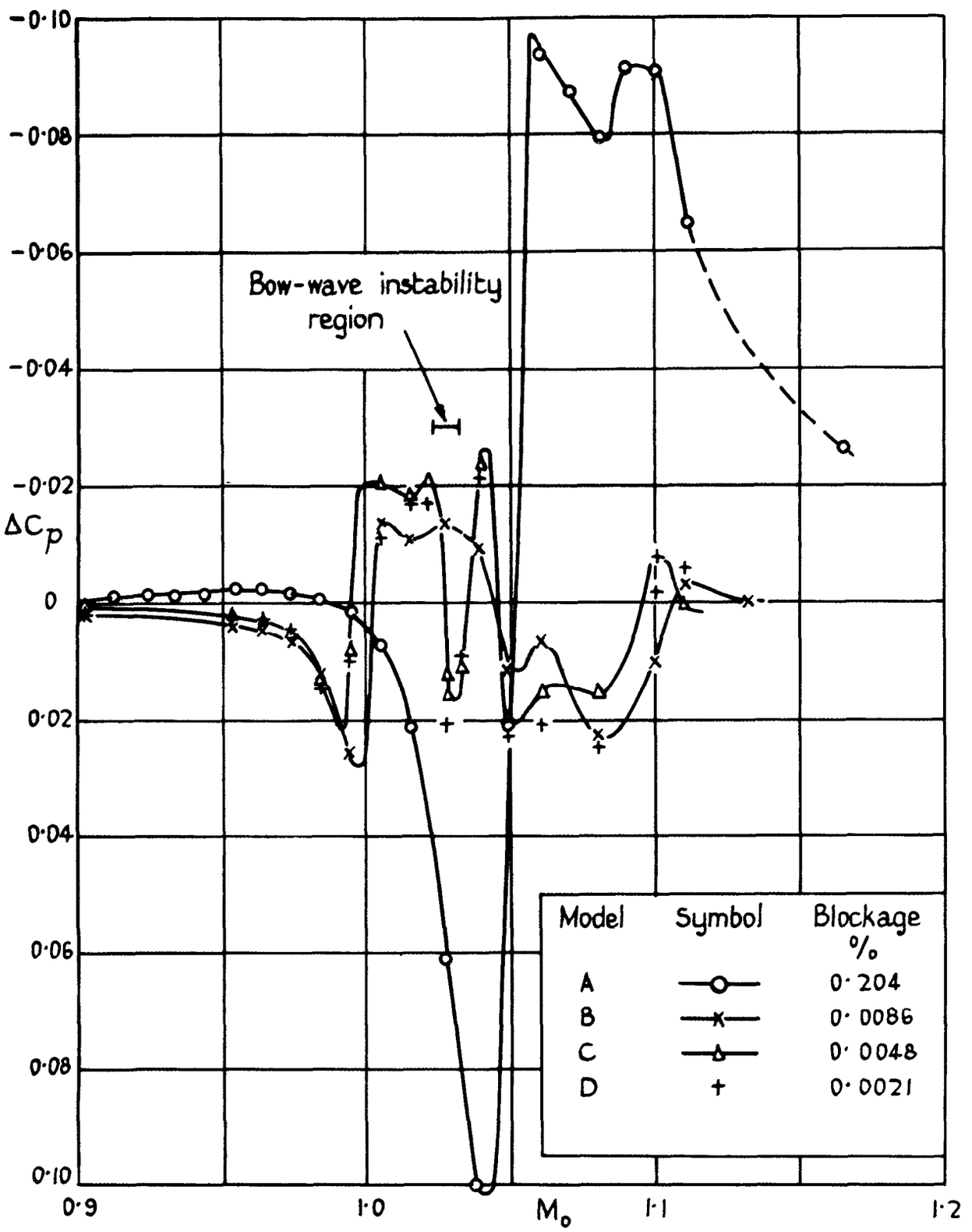

Static pressure changes measured by the four Mark IX A-type models.

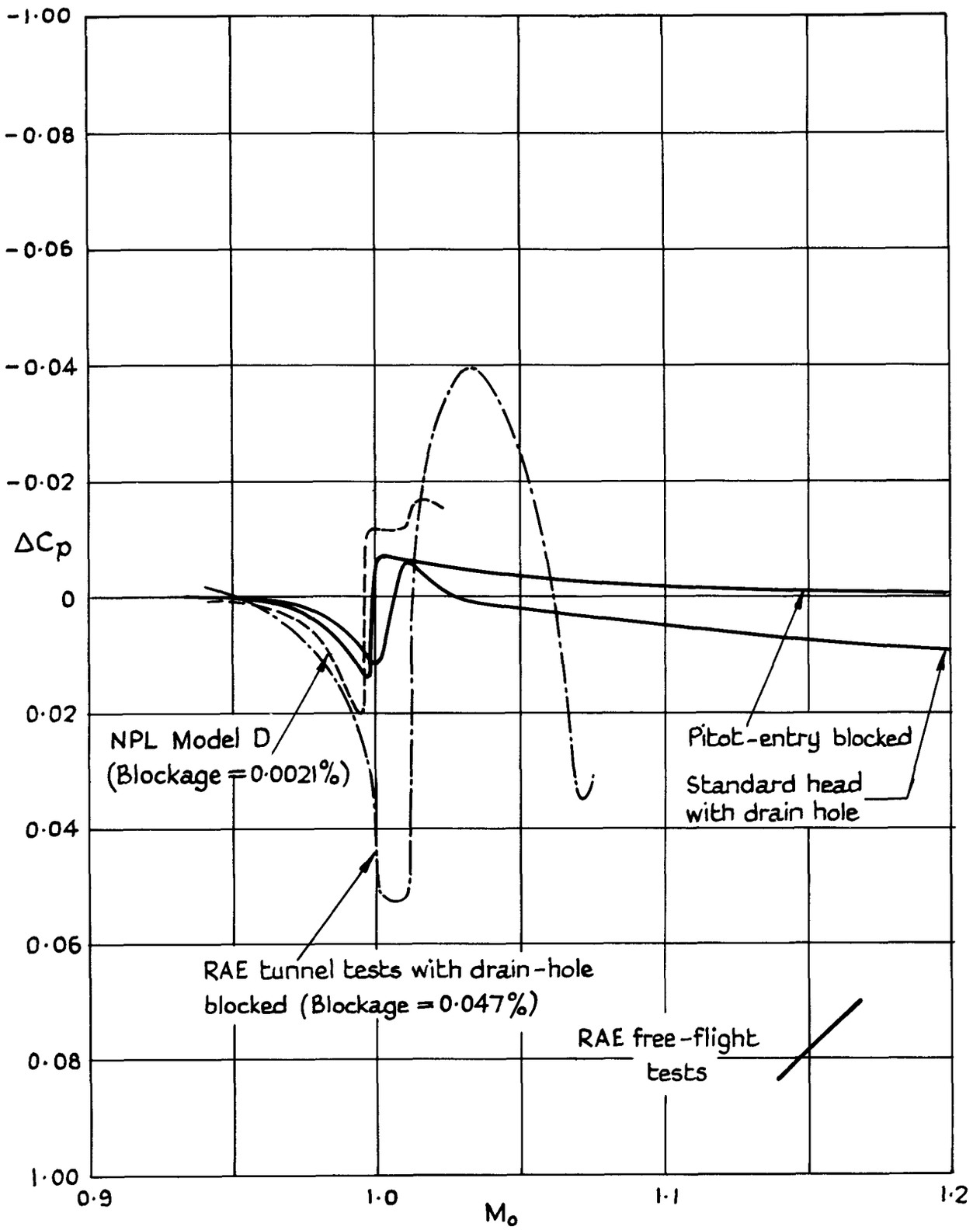

Comparison of different results from Mark IX A -type models

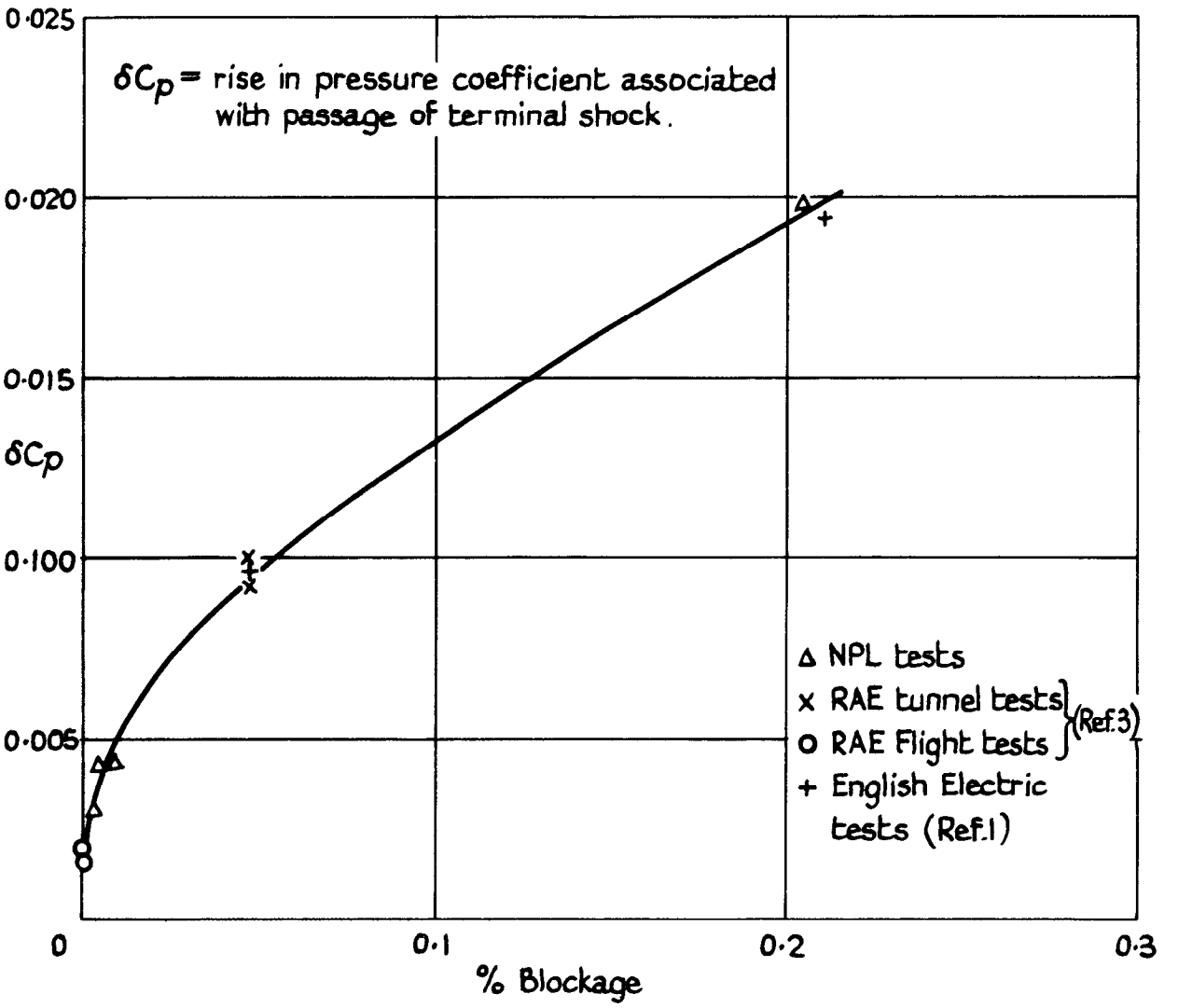

Effect of blockage on pressure-rise measurement with Mark IX A type tubes

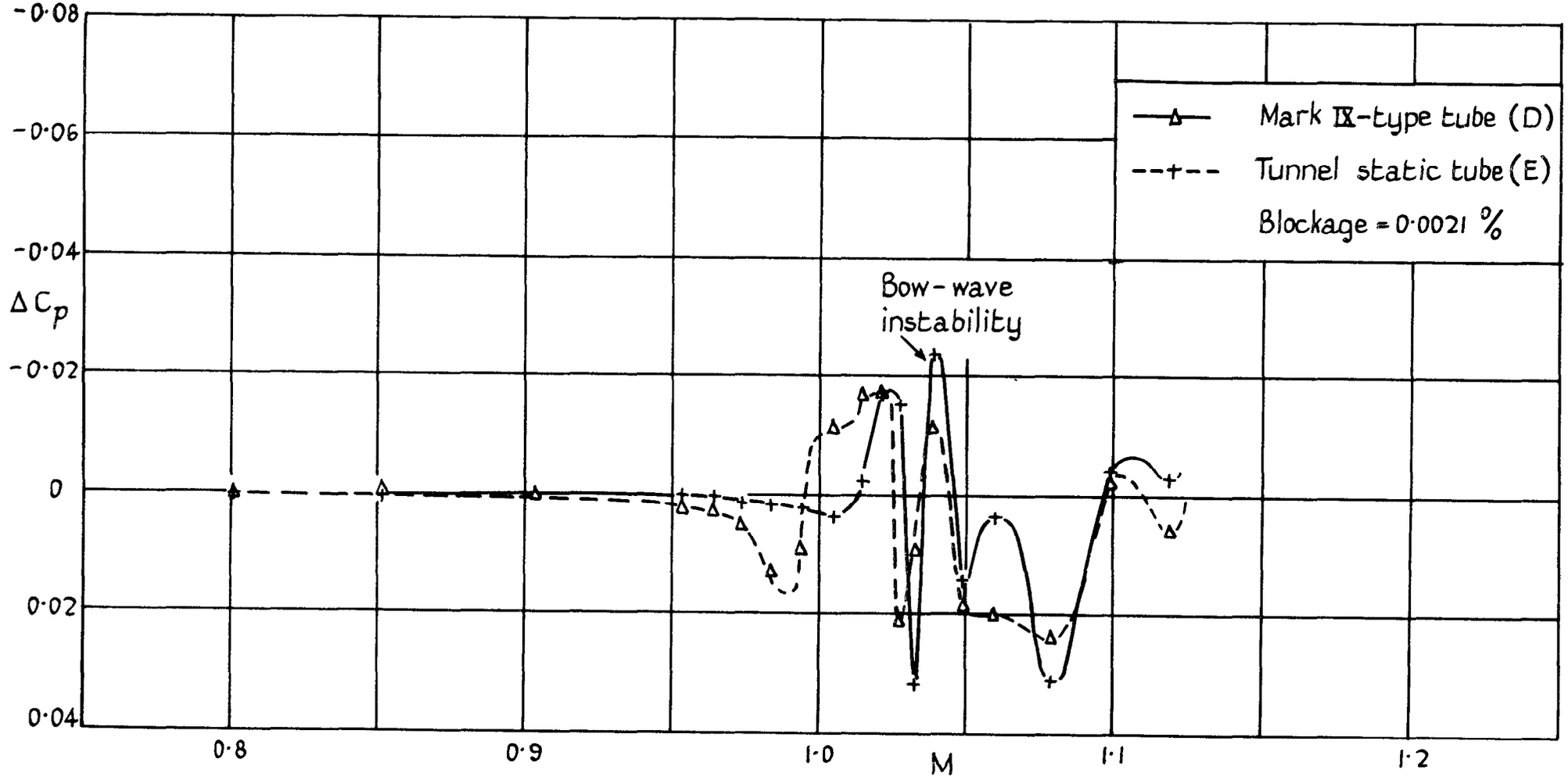

Comparison between tunnel static tube and smallest Mark IX A type static tube.

C.P. No. 430
(20,306)
A.R.C. Technical Report

Printed and published by
HER MAJESTY'S STATIONERY OFFICE

To be purchased from
York House, Kingsway, London W.C.2
423 Oxford Street, London W.1
13A Castle Street, Edinburgh 2
109 St Mary Street, Cardiff
39 King Street, Manchester 2
Tower Lane, Bristol 1
2 Edmund Street, Birmingham 3
80 Chichester Street, Belfast
or through any bookseller

Printed in Great Britain

S.O. Code No. 23-9011-30

C.P. No. 430